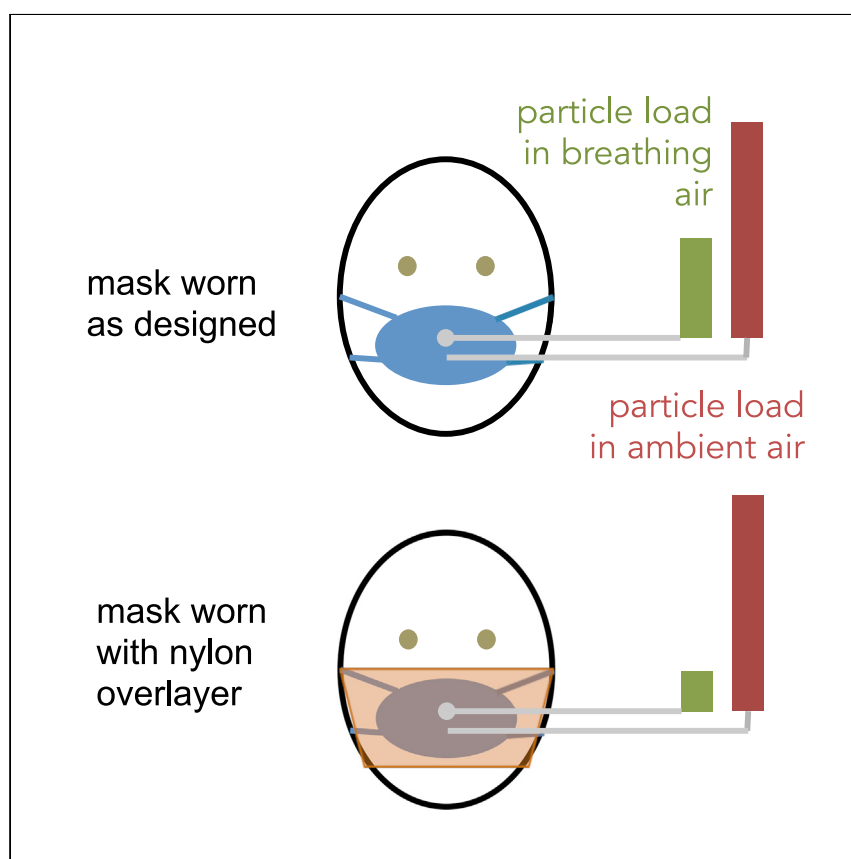## Article

Quantitative Method for Comparative Assessment of Particle Removal Efficiency of Fabric Masks as Alternatives to Standard Surgical Masks for PPE

particle load
in breathing
air

mask worn
as designed

particle load
in ambient air

mask worn
with nylon
overlayer

Amy V. Mueller, Matthew J. Eden, Jessica M. Oakes, Chiara Bellini, Loretta A. Fernandez

l.fernandez@northeastern.edu

HIGHLIGHTS

Surgical masks removed 53%–75% of particles <300 nm from air when worn as designed

Cloth masks ranged in particle removal efficiency from 28% to 91% when worn as designed

A nylon overlayer improved particle removal efficiency of many masks by minimizing gaps

Cloth masks are being used to control the spread of SARS-Cov-2 virus, but the efficacy of these masks is not well known. Here, tools and methods typically used to assess tight-fitting respirators were modified to quantify the efficacy of fabric masks at removing small aerosol particles (<300 nm) from breathing air. Both commercial surgical masks and cloth masks had widely varying effectiveness (53%–75% and 28%–91% particle removal, respectively). Surgical-style mask efficacy generally improved with addition of an elastic nylon overlayer.

Development

6

Practical, real world, technological considerations and constraints

Article

Quantitative Method for Comparative Assessment of Particle Removal Efficiency of Fabric Masks as Alternatives to Standard Surgical Masks for PPE

Amy V. Mueller,[1] Matthew J. Eden,[2] Jessica M. Oakes,[2] Chiara Bellini,[2] and Loretta A. Fernandez[1,3,*]

SUMMARY

In response to the COVID-19 pandemic, cloth masks are being used to control the spread of virus, but the efficacy of these loose-fitting masks is not well known. Here, tools and methods typically used to assess tight-fitting respirators were modified to quantify the efficacy of community-produced and commercially produced fabric masks as personal protective equipment. Two particle counters concurrently sample ambient air and air inside the masks; mask performance is evaluated by mean particle removal efficiency and statistical variability when worn as designed and with a nylon overlayer, to independently assess fit and material. Worn as designed, both commercial surgical masks and cloth masks had widely varying effectiveness (53%–75% and 28%–91% particle removal efficiency, respectively). Most surgical-style masks improved with the nylon overlayer, indicating poor fit. This rapid testing method uses widely available hardware, requires only a few calculations from collected data, and provides both a holistic and aspect-wise evaluation of mask performance.

INTRODUCTION

In response to the critical shortage of medical masks resulting from the COVID-19 pandemic, large portions of the population are mobilizing to produce cloth masks using locally sourced fabrics. While the general population is being advised to wear masks to protect others from virus that may be spread from the wearer, the efficacy of these masks as a means of protecting the wearer from airborne particles carrying virus is also a concern, particularly as medical masks grow scarce. This issue may become more critical if it becomes necessary for medical care workers to use similar alternative personal protective equipment (PPE),[1] but is already important for individuals who may be caring for a household member who is ill or who may be in a high-risk category for complications.[2]

The effectiveness of masks to protect wearers from airborne particles is known to be a function of both materials and fit. Standard methods to test the performance of respirators and masks designed to form a seal against the face, such as N95 respirators, assume that appropriate high-filtration materials have been used in the construction of the masks and therefore employ instruments that test the fit by comparing the concentration of particles in air inside and outside of the mask while the subject moves his/her head through a series of positions.[3] Several instruments have been specifically designed to perform these tests (e.g., the TSI PortaCount), simplifying the testing process for users by reporting a single metric of "fit" (i.e., Fit Factor = ratio of time-averaged particle concentration outside and inside mask). In contrast,

Progress and Potential Statement

This work was initiated in response to the need to understand the potential personal protective benefits of commercially produced and homemade masks for use during the COVID-19 pandemic. Understanding that the specialized equipment required to measure filtration efficiency of mask materials for the most penetrating particle size (usually around 300 nm) is not widely available and that the protection provided by any mask is dependent on the mask fit at well as materials, we sought to develop a method for rapidly assessing new mask designs using readily available instrumentation. The methods described in this work may be used to help home in on materials, construction techniques, and designs that are most effective at removing small (<300 nm) non-oil aerosol particles from air breathed through a mask. If applied broadly to a large set of masks, best practices for constructing, cleaning, and wearing masks with the goal of protecting public health may be found.

standard methods for surgical masks focus exclusively on testing the materials and do not provide for a measurement of the mask as constructed or as worn.[4–7]

Anticipating the need to produce face coverings from readily available materials, several studies have used these standard methods for materials testing to compare the particle removal efficiency of materials such as cotton T-shirts, sweatshirts, handkerchiefs, and towels with the particle removal efficiency of materials used to manufacture facepiece respirators (N95 masks) and surgical masks.[8–10] Furthermore, tools developed for N95-type masks have been applied directly to evaluate particle filtration for loose-fitting, surgical-type masks.[11] Generally, these studies have found that no commonly available materials produce particle removal efficiency close to respirators such as N95s, with cotton cloth facemasks providing about half the protection (i.e., Fit Factor decrease by a factor of 2) of standard surgical masks against airborne particles.[11] Notably, these previous studies were unable to pinpoint the problems with loose-fitting masks (i.e., separate out a poor fit from poor materials used in the construction), although in other work an elastic layer (e.g., nylon stocking) placed over the mask when worn has been found to improve particle removal efficiency of loose-fitting masks by minimizing air flow around the cloth layers.[12]

Importantly, it has been shown that head motions and positions do not significantly affect the performance of loose-fitting masks in terms of filtering out nanosized particles,[11] suggesting that a simplified mask-testing protocol (compared with the multi-step fit test used for respirators) may be sufficient for characterizing particle removal efficacy of loose-fitting masks. Given the highly varied results and protocol shortcomings noted for prior studies,[13] development of a rapid and quantitative method for evaluating potential PPE options would be of great value to the general public at this time.

The purpose of this work was to develop a standardized method to quantitatively assess the efficacy of sewn fabric facemasks and standard surgical masks in terms of protecting the wearer from airborne particulates of the size range associated with aerosolized SARS-CoV-2 virus (<10 μm), hypothesized to be important in transmission from asymptomatic or pre-symptomatic carriers.[14] This leverages widely available instrumentation designed for respirator fit testing, but provides two key adjustments that improve the data quality for loose-fitting mask testing. First, two instruments are used to simultaneously record high-resolution (1 Hz) particle concentration measurements in the room and behind the mask, enabling the method to be used in cases where particle concentration may vary on the timescale of tests, in comparison with standard fit testing, which requires large differences in particle concentrations in the room and behind the mask (approximately two orders of magnitude) but are not affected by smaller variations in ambient particle concentration (Figure 1). Data recorded during experiments described below show variability of particle concentrations by up to a factor of 2 over <1 min, supporting the need for this dual-instrument configuration if used outside of specialized testing rooms. Second, by conducting separate tests for masks worn loosely (as designed) and for the masks held close to the face using a layer of nylon stocking (as recommended by Cooper et al.[12]) (Figure 2), the method enables independent evaluation of the mask fit and mask materials as they contribute to overall particle removal efficiency.

The proposed protocol enables testing of an individual mask design (n = 3 masks for statistical analysis) within ~30 min for systems with digital data collection, providing a rapid screening tool to test a variety of mask designs produced from readily available materials. To validate the methodology, we report here the data collected from

[1]Departments of Civil and Environmental Engineering and Marine and Environmental Science, Northeastern University, Boston, MA 02115, USA

[2]Department of Bioengineering, Northeastern University, Boston, MA 02115, USA

[3]Lead Contact

*Correspondence:
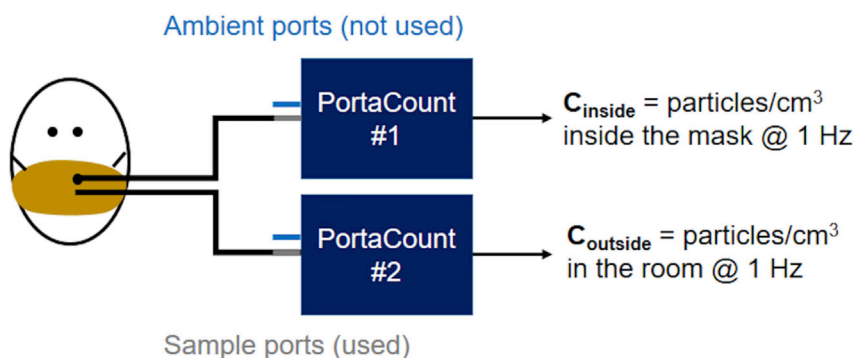l.fernandez@northeastern.edu

Figure 1. Schematic Diagram of Testing Setup

Test setup has two PortaCount systems running in parallel; 1/8″ diameter tubing of identical length connects (top) the mask port to one instrument sampling port and (bottom) a tube inlet located just outside the mask to the second instrument sampling port. Both instruments are run in "Count" mode whereby concentrations are reported once per second (1 Hz). The dual-instrument configuration is required because each instrument has only one internal measurement cell, for which the input is swapped between the sampling and ambient inputs during standard fit testing. Photograph of PortaCounts used, including ports and tubing, is provided in Figure S1.

an initial set of commercial and homemade masks, although results from ongoing tests are being updated regularly at a public web portal as additional prototype masks are evaluated (see Supplemental Information). Given the limited time and current social distancing precautions, all tests were conducted while masks were being worn by the same subject, breathing normally, through the nose, with the mouth closed, while holding the head at a steady position. Data reported by van der Sande et al.[11] provide confidence that limitation of motions and positions does not significantly limit the conclusions that can be drawn from the resulting data, and results from a single test subject are used here primarily to validate the protocol itself.

RESULTS AND DISCUSSION

The percent removal of particles (of size range characterized below, $D_p < 300$ nm) (Figure 3) for each mask was computed from data collected each second over 1-min tests; examples of the high-resolution data collected for each test are provided in Figure 4 for a well-fitted N95 mask (N95-1) and a surgical-style cloth mask (CS-1). The breathing pattern of the wearer can be observed as oscillations in the "inside mask" data. The particle count while wearing the N95 respirator is likely dipping during inhalation as air is filtered through the mask and rising as particles are exhaled (<100 p/cc, based on three replicate mask tests). The sawtooth pattern for the loose-fitting mask, however, is likely peaking on the inhale as particle-laden air is pulled around the mask and dipping on the exhale as lower particle air from the lungs blends with air inside the mask. The issue of variability in ambient particle concentrations over a 1-min test is clearly visible in the top of Figure 4.

From these data, one can extract both mean removal efficiency and a measure of time-based variation ($\bar{x}$ and s_t, as defined below), which each provide information on mask performance. It is observed that $\bar{x}$ and s_t are inversely correlated (Figure 5), whereby an improved fit generally leads to both higher mean particle removal efficiency and lower time-based standard deviation (consistency in particle removal), independent of the materials being used.

Data collected with the subject wearing the nylon overlayer alone had $\bar{x} = 7.0\% \pm 2.5\%$ (standard deviation calculated from n = 3 replicates) with $s_t = 18\%$; it is

Figure 2. Example of Facemask and Nylon Overlayer Used in Tests

Facemask (Mask CS-1) worn as designed (A) and with a nylon overlayer (B) with tightly sealed grommet positioned at the philtrum of the upper lip. The grommet is used to sample air from inside the mask during testing. Note that: this mask could have been worn inside-out to ensure the folds faced down. However, for the purposes of this test, precautions against particle collection in folds were not considered necessary.

concluded, therefore, that the overlayer itself does not provide significant particle removal, and in the following discussion it is considered primarily to improve the snugness of fit of the underlying mask. In addition, aerosol neutralizers and dryers are not used with the TSI PortaCount and its accompanying particle generator. Thus, masks with charged fibers may yield greater particle removal using this method than would be observed using methods and instruments that test only uncharged, dry particles.

The method is first evaluated through analysis of available commercial masks (Figure 6), including N95 respirators, surgical masks marketed for medical use, and others (in this case, a surgical-style mask with a charcoal-embedded layer marketed for persons with allergies or wearing while exercising in areas with high levels of air pollution). Blue bars in Figure 6 show mean particle removal percentage for masks worn as designed, while gray bars provide a proxy for best possible fit by adding the nylon overlayer. Differences between blue and gray bars provide a measure of the looseness of the fit (extent of leakage of air around the mask in normal wear) while gray bars provide a measure of particle removal capacity of the mask material.

As expected, the mean removal efficiency for the well-fitted N95 mask (N95-1) is greater than 99%, with very low variability between replicates ($s = 0.36\%$) and low time-based standard deviation ($s_t = 0.78\%$, see Figure 5 data point with highest particle removal efficiency). This corresponds to a Fit Factor ($C_{outside}/C_{inside}$) of 126, which is above the minimum passable standard of 100;[15] however presentation of results as mean and variability provides more information on the range of particle removal efficiencies experienced by the user. The poorly fitted N95 mask (N95-2) has a lower mean removal efficiency ($\bar{x}=90.6\%$), higher variability between replicates ($s = 5.9\%$), and higher time-based standard deviation ($s_t = 4.6\%$). This corresponds to a fit factor of 10.6, which is below the minimum passable standard.

In comparison, the standard medical-type masks (S-1 to S-3), when worn over the chin and with an adjusted nose wire, had a mean removal efficiency of only
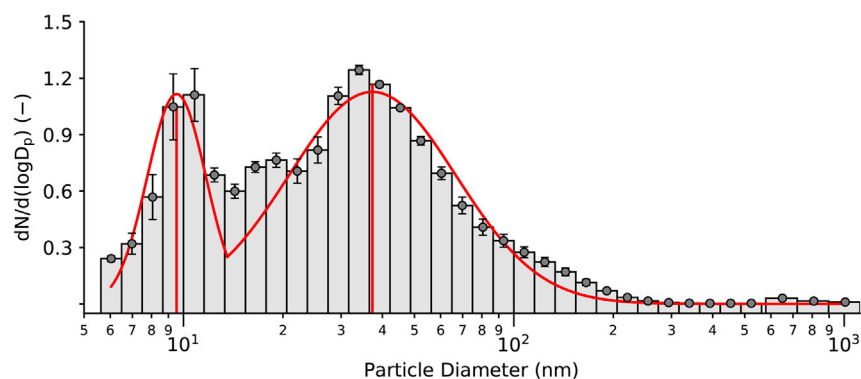
Figure 3. Particle Size Distribution in Ambient Air

Average histograms of normalized particle frequency as a function of size, with superimposed bimodal lognormal distribution. Count median diameter (CMD $\pm$ 95% CI) is 9.53 $\pm$ 2.19 nm for the first peak and 37.30 $\pm$ 15.40 nm for the second peak. Geometric standard deviation (GSD $\pm$ 95% CI) is 1.23 $\pm$ 0.13 for the first peak and 1.79 $\pm$ 0.44 for the second peak. Particles generated by the TSI Particle Generator account for the larger peak, while particles in lab air account for the smaller peak.

50%–75% when worn as designed. In comparison, when tightly fitted to the face using a nylon overlayer, these masks achieve from 86% to 90% mean removal efficiency, indicating that (1) the material can actually provide much better filtration than is achieved in normal wear and (2) differences between brands are primarily in the quality of fit rather than the quality of material used. Interestingly, in this case the carbon filter mask (O-1) performs approximately as well as the best-performing surgical mask despite a significant difference in the design specifications and materials used.

The same measurements and metrics were then used to test 15 different cloth masks made by or being marketed to the public at this time (April to May 2020). Results (Figure 7) are presented as absolute particle removal efficiency (top) and in comparison with the top-performing surgical mask (S-1) (bottom), which the cloth masks are expected to replace outside of medical settings. While these masks represent a small subset of available masks and materials, several useful preliminary observations can be made.

First, the quality of cloth masks is highly variable, both in fit (difference between blue and gray bars) and material particle removal capacity (gray bars); therefore, the public would greatly benefit from a quantitative method for evaluating masks they may be considering for health-protective reasons. Second, it appears that different mask shapes may provide a more consistent fit even when hand-made using standard patterns; for example, in these data the cone masks appear generally to fit better than the surgical-style masks (as evaluated by difference between blue and gray bars in Figure 7, where addition of the nylon layer generally improved performance for surgical-style masks but not for cone-shaped masks). Exceptions to improvement when adding the nylon overlayer were rare and due to material stiffness whereby the mask could not completely conform to the wearer's face and therefore the nylon layer led to bunching (creation of new air-leakage pathways). The nylon layer also reduced the variability with time, as indicated by a decrease in the time-based standard deviation. Both of these metrics indicate improved protection for the wearer from particle inhalation.

When using mask S-1 worn as designed as a baseline, several of the cloth masks match or exceed this performance (Figure 7, bottom). The masks that achieved
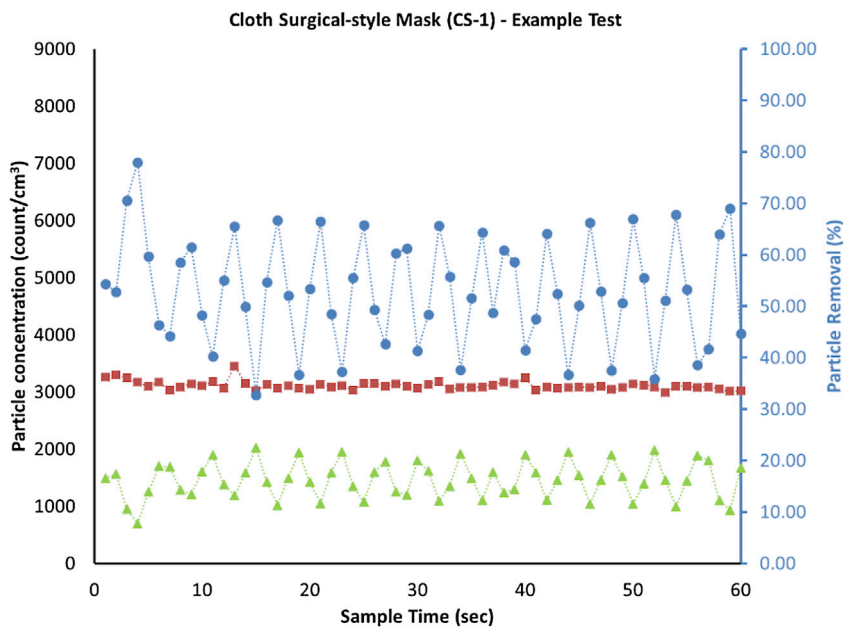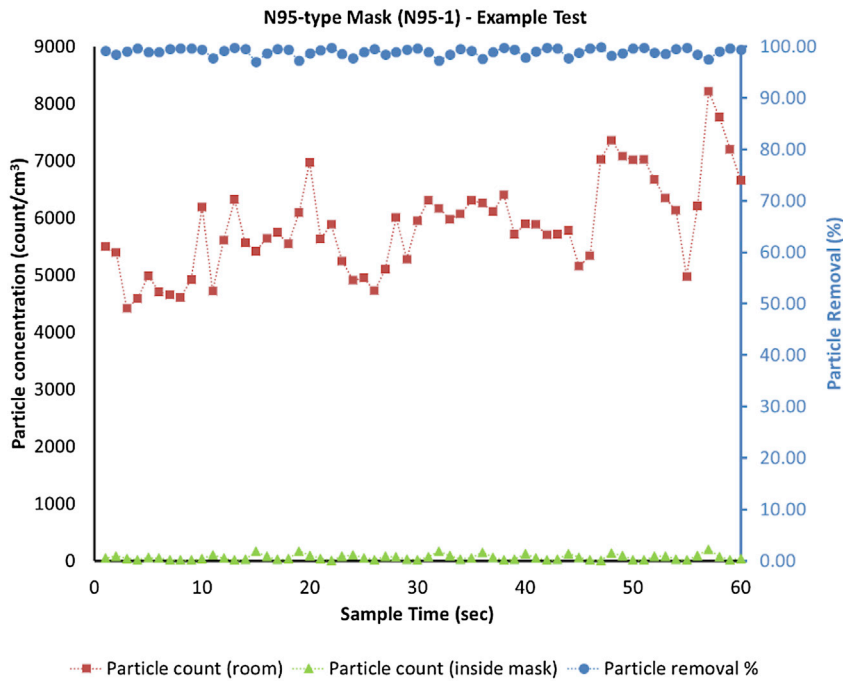
Figure 4. Examples of High-Resolution Data Collected Using PortaCount

Particle concentrations in the room (red squares) and inside the mask (green triangles) with calculated removal percentage (blue circles) versus time for a single 1-min test of a well-fitted N95 mask (N95-1, top) and an example cloth surgical-style mask (CS-1, bottom). Time-based variability in particle removal efficiency corresponds to the breathing patterns of the mask wearer (inhales versus exhales). As expected, the N95 mask has high and consistent particle removal efficiency ($\bar{x}$=99.0%, s_t = 0.75% for this single test). The cloth surgical-style mask has both lower particle removal efficiency and higher variability ($\bar{x}$=53.0%, s_t = 10.5% for this single test).
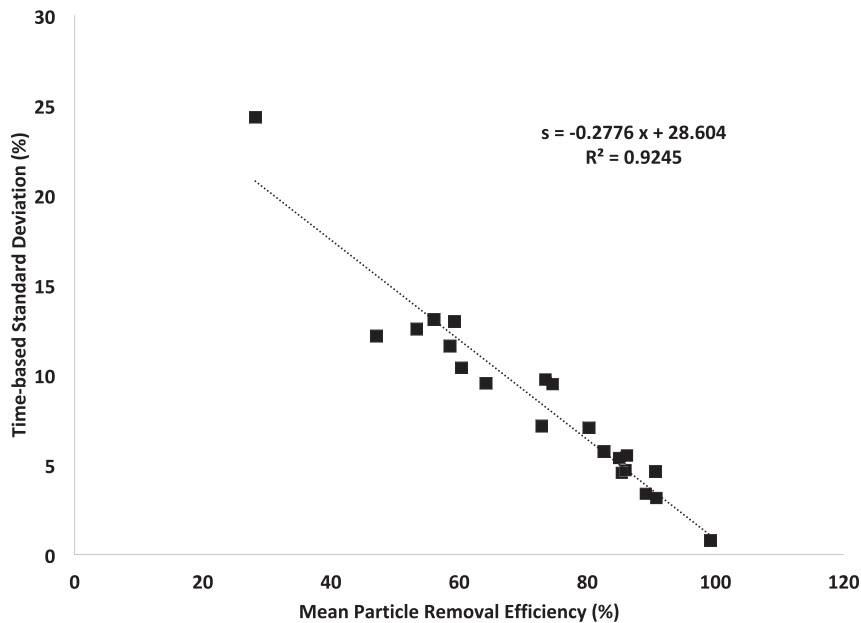
Figure 5. Linear Correlation between Mean Particle Removal Efficiency and Standard Deviation of the Measurement

Improving mask performance through better fit and filtration materials leads both to increased mean particle removal efficiency and decreased variation in filtration over time; data shown for masks worn as designed.

this level of filtration without the nylon overlayer were cone shaped and included a layer of meltblown filter fabric, similar to interfacing fabric being added to many homemade masks, and specified as BFE85, between fabric cover layers. Additional filter layers, including water-repellent non-woven cloth marketed as disposable massage table covering and dry disposable baby wipes, improved the particle removal efficiency only moderately in the cone-shaped masks. Surgical-style masks that achieved the best particle removal efficiency with the addition of a nylon overlayer included a filter layer (organic cotton batting, interfacing fabric, or loosely woven cotton muslin) between two layers of cotton fabric. These data are not included here due to the limited number of replicates but are available on a web portal (Supplemental Information).

Conclusion

A rapid testing protocol is presented for evaluation of loose-fitting type masks to provide quantitative, intercomparable data for particle removal efficacy of masks made with different types of fabrics and with different designs/fits, independently providing an assessment of the quality of the mask fit and the material used. The protocol collects high-resolution particle-count data inside and immediately outside of masks to report both mean and time-based standard deviation of particle removal efficiency while wearing the mask as designed and under a nylon layer that snugs the mask to the face. The protocol is validated on a well-fitted N95 mask, and a commercial surgical-type mask is used as a reference baseline for evaluation of alternative mask particle removal efficiencies. Commercial surgical masks marketed for medical use had mean particle removal efficiencies from 53% to 75% when worn as designed but up to 90% when snugged to the face under a nylon layer. Cloth masks tested had widely varying mean particle removal efficiencies (<30% to 91%), with some cloth masks achieving particle removal efficiencies similar to those of commercial surgical masks. However, in general, surgical-style cloth masks had poor fit (i.e., performance
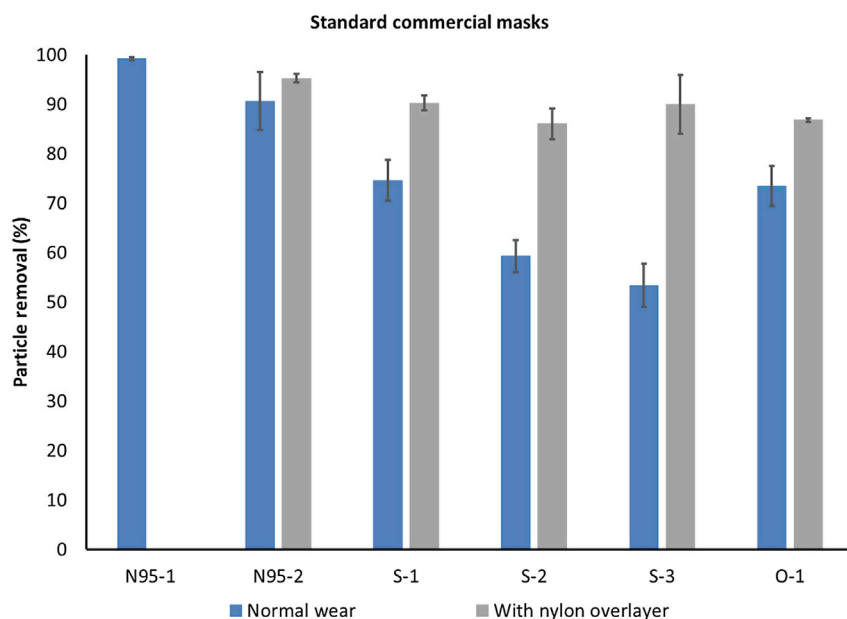
Standard commercial masks

Figure 6. Performance of Commercially Available Masks and Respirators
Particle removal efficiency of standard commercial masks of three types: N95 (N95-n), surgical style marketed for medical use (S-n), and other (O-1, a charcoal filter mask). Data collected with a nylon overlayer holding the mask in place represent a proxy for best possible fit, i.e., gray bars provide a measure of the particle removal capacity of the materials. N95-1 was well fitted to the mask wearer and shows the expected >99% filtration, while N95-2 was less well fitted, as seen by the difference between the blue and gray bars. While the fit of the three surgical masks (S-1 to S-3) is quite different (blue bars), the materials are comparable (gray bars). Error bars show standard deviation between replicates (n = 3 masks for each type tested).

was greatly enhanced with the nylon overlayer) compared with cone-shaped masks, and masks with higher particle removal efficiency tended to have a filter layer (e.g., meltblown BFE85 filter layer) in addition to two layers of cotton or non-woven fabric. This rapid testing method (~30 min per mask design including replicates for statistical validity) provides a holistic evaluation of mask particle removal efficacy (material, design, and fit) while enabling independent evaluation of these characteristics.

EXPERIMENTAL PROCEDURES

Resource Availability

Lead Contact
Loretta Fernandez, l.fernandez@northeastern.edu.

Materials Availability
This study did not generate new or unique reagents.

Data and Code Availability
All experimental data are available upon reasonable request to the Lead Contact author.

Particle Counters
Particles in ambient air and air inside of the mask breathing zone were counted using two PortaCount Plus Model 8028 instruments running in count mode. The PortaCount Plus instrument uses a condensation particle counter to determine particles per cm^3 in air sampled at a flow rate of 1.67 cm^3/s and reports one value (in

A

Particle removal rate: Cloth masks of 3 styles

B

Cloth mask performance relative to commercial Mask S-1
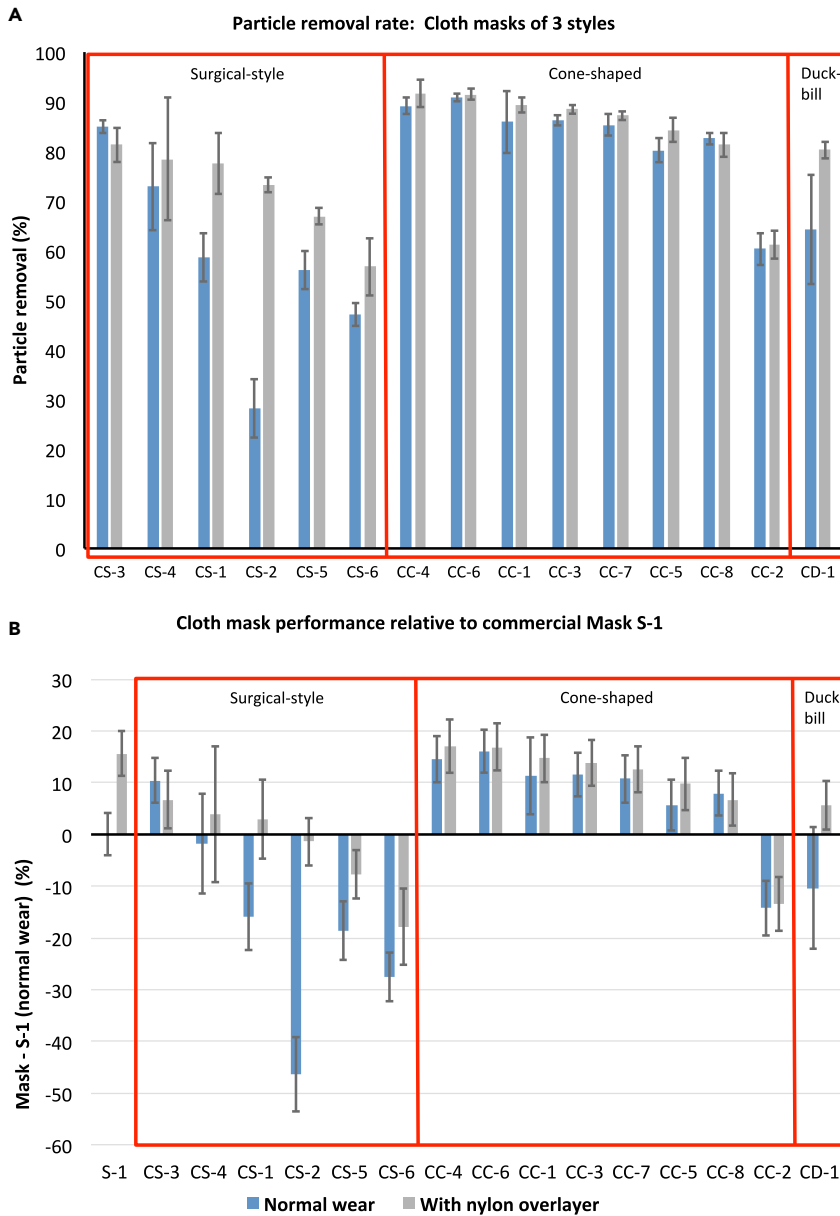
■ Normal wear ■ With nylon overlayer

Figure 7. Performance of Cloth Masks and How They Compare with a Standard Surgical Mask
Performance of a range of cloth masks being made by the community and by commercial vendors presented as absolute performance (A) and in comparison with S-1, the top-performing surgical mask (B). Preliminary data show the difference between performance of masks using different form factors, e.g., cone-shaped masks appear to have a better and more consistent fit to the face. Notably, multiple cloth masks perform as well as or better than surgical masks when worn as designed, and some provide particle removal equivalent to that of surgical masks snugged to the face. However, there is wide variability in particle removal provided by cloth masks, due to both fit (difference between blue and gray bars) and materials (gray bars). Error bars show SD between replicates (n = 3 masks for each type tested).

particles/cm^3) each second.[16] The instrument counts particles ranging in size from 0.02 to >1 μm; however, data on the size distribution of counted particulates is not reported. Size distribution of the particles used to challenge the masks was therefore measured independently, as reported in the following section.

Mask fit testing is usually conducted using a single instrument in fit test mode, which sequentially tests air inside and outside the mask and therefore depends on an assumption of consistent particle concentration in the room. As this assumption was frequently violated in our test setup even in cases where particle generation was used, two PortaCount instruments were used in count mode to simultaneously collect and display continuous data for ambient air and inside mask air at high frequency (1 Hz) during minute-long tests.

Two tubes of 1/8″ inner diameter (sold with the PortaCount Instrument) and trimmed to equal length (approximately 100 cm) sampled air just inside and outside of the mask. Air inside the mask was sampled through a tight-fitting grommet inserted into each mask using a TSI Fit Test Probe Kit (model 8025-N95) and positioned at the philtrum of the upper lip per standard mask-testing guidance appropriate to the shape of each mask. Ambient air was sampled from a position ∼3 cm from the grommet on the outside of the mask.

Particle Generation and Characterization

All tests were run in a 65-m^3 rectangular room after at least 15 min of operating a TSI Particle Generator Model 8026 (TSI, Shoreview, MN, USA). This tool is typically used in conjunction with TSI PortaCount instruments to ensure sufficiently high particle counts and appropriate size distributions to meet Occupational Safety and Health Administration (OSHA) standards. Particles were generated from a dilute (2%) solution of sodium chloride (NaCl), reported to have a nominal size of 40 nm with a geometric standard deviation of 2.2 based on instrument specifications.[17] To verify that the particles challenging the masks were composed primarily of these generated particles, the particle size distribution in the room was characterized by running three 5-min tests approximately hourly on several testing days (n = 21 in replicates of three) using the TSI Engine Exhaust Particle Sizer Spectrometer Model 3090 (for particles in the range 5.6–560 nm, with 32 channels acquired at 10 Hz) and the TSI Optical Particle Size Spectrometer Model 3330 (for particles in the range 0.3–10 μm, with 16 channels acquired at 1 Hz). The size distribution of particle number concentration was consistent at all times and days sampled, which supported the averaging of collected data. The histogram of average normalized particle frequency revealed a bimodal distribution of particle sizes, shown in Figure 3. Confidence intervals (CI) for the count median diameter (CMD) and the geometric standard deviation (GSD) were calculated from Student's t test statistics, with p = 0.05 and M = 20 degrees of freedom. The first peak likely represents particles that are not filtered by building HVAC (heating/ventilation/air-conditioning) systems, as the distribution parameters (CMD = 9.53 ± 2.19 nm, GSD = 1.23 ± 0.13; average ± 95% CI) are consistent with background air measurements reported by the authors in other rooms and buildings on campus.[18] Features of the second peak (CMD = 37.30 ± 15.40 nm, GSD = 1.79 ± 0.44) are in agreement with specifications reported for the TSI Particle Generator manual. Overall, 97.01% ± 0.02% (average ± 1●s) of particles are in the standard range used to challenge masks (<300 nm), so the reported particle removal efficiencies can be directly compared with numbers reported to comply with OSHA standards.

Calibration

An inter-calibration was conducted between the two PortaCount modules to account for any drift or changes in calibrations due to, e.g., wick saturation. Each sampling day, calibration data (a minimum of three 1-min time series, n = 180) were collected by recording readings simultaneously on both instruments while sample tubes were side by side (within 3 cm), open to the air (no mask), and a minimum of 1 m from any person and 2 m from the particle generator (as recommended by the manufacturer). Correlation coefficients between the readings from the two instruments were consistently above 0.9,

and day-specific linear regressions were used to normalize particle counts from the Reference PortaCount to equivalent particle counts from the Mask PortaCount before calculating particle removal efficiencies.

Data Collection and Processing

Each mask test consisted of three 1-min runs while wearing the mask as designed (Figure 2A). In addition, the mask material was held against the face by adding a section of nylon stocking over the entire mask area following recommendations from Cooper et al.[9] (Figure 2B) to simulate best possible fit and provide information on material filtration, and a single 1-min test was recorded in this configuration. All masks except the well-fitted N95 were tested in this second configuration. Results are reported only for masks for which at least three replicate sample masks were available (data for masks with n < 3 are being provided through our web portal; see Supplemental Information).

Particle concentration data from inside and outside the mask was logged each second for the 1-min tests using video capture and subsequently transcribed to a database (noting that newer PortaCount models can log count data through a software interface to simplify data collection). Particle removal at each time step was calculated as follows:

$$\% \text{ particle removal} = \text{PPR} = \frac{C_{outside} - C_{inside}}{C_{outside}} \times 100, \quad \text{(Equation 1)}$$

where $C_{outside}$ is the corrected reading from the Reference PortaCount (as described above) and C_{inside} is the reading in the breathing zone of the mask.

Average particle removal efficiency ($\overline{x}$, reported as percent removal), standard deviation between masks (generally n = 3, s reported as percentage), and mean standard deviation over the 1-min tests (s_t, reported as percentage) were computed for each mask with and without a nylon overlayer. These summary statistics can be used to calculate Fit Factor for the masks, if desired, using Equation 2:

$$\text{Fit Factor} = \frac{C_{outside}}{C_{inside}} = \frac{1}{1 - \text{PPR}/100}. \quad \text{(Equation 2)}$$

Masks

Masks tested are given labels according to the mask type and then an individualized sample number. Commercial masks are divided into N95 type (N95-1, N95-2, and so forth), surgical-style (S-1 and so forth), and other (O-1 and so forth) masks. Cloth masks are given a pre-pended "C" identifier and divided into surgical-style (CS-1 and so forth), cone-shaped (CC-1 and so forth), and duck-bill-shaped (CD-1 and so forth) masks (Figure S2). Results are reported for a range of commercially produced, medical-type facemasks (masks with elastic ear loops and in-sewn wires to adjust fit to the bridge of the nose), and 15 sewn fabric facemasks of various designs that were sourced from community volunteers producing masks for essential personnel as well as online vendors that have started to market masks of this type since March 2020 (Table S1). Several of the fabric masks included filter layers such as non-woven polypropylene fabric, meltblown textiles, and disposable baby wipes. In addition, several sewn masks included hydrophobic layers including interfacing (Pellon) and non-woven fabric marketed as disposable massage table covering. Some masks included wires to fit the masks across the bridge of the nose. A set of well-fitted (N95-1) and poorly fitted (N95-2) masks were tested to validate the protocol.

SUPPLEMENTAL INFORMATION

ACKNOWLEDGMENTS

AUTHOR CONTRIBUTIONS

Conceptualization, L.A.F. and A.V.M.; Methodology, L.A.F., A.V.M., C.B., and J.M.O.; Formal Analysis, A.V.M. and C.B.; Investigation, L.A.F., A.V.M., M.J.E., J.M.O., and C.B., Writing – Original Draft, L.A.F., A.V.M., and C.B.; Writing – Review & Editing, A.V.M., C.B., and L.A.F.

DECLARATION OF INTERESTS

The authors declare no competing interests.

REFERENCES

1. MacIntyre, C.R., Seale, H., Dung, T.C., Hien, N.T., Nga, P.T., Chughtai, A.A., Rahman, B., Dwyer, D.E., and Wang, Q. (2015). A cluster randomised trial of cloth masks compared with medical masks in healthcare workers. BJM Open 5, e006577.

2. MacIntyre, C.R., Cauchemez, S., Dwyer, D.E., Seale, H., Cheung, P., Browne, G., Fasher, M., Gao, Z., Booy, R., and Ferguson, N. (2009). Face mask use and control of respiratory virus transmission in households. Emerging Infect. Dis. 15, 233–241.

3. OSHA (1998). Respiratory Protection, 29 (Occupational Safety and Health Administration (OSHA), Department of Labor), CFR Parts 1910 and 1926.

4. ASTM (2019). Standard Specification for Performance of Materials Used in Medical Face Masks (ASTM International), Standard F2100-19.

5. ASTM (2017). Standard Test Method for Resistance of Medical Face Masks to Penetration by Synthetic Blood (Horizontal Projection of Fixed Volume at a Known Velocity) (ASTM International), Standard F1862/F1862M-17.

6. ASTM (2019). Standard Test Method for Evaluation of the Bacterial Filtration Efficiency (BFE) of Medical Face Mask Materials, Using a Biological Aerosol of *Staphylococcus aureus* (ASTM International), Standard F2101-19.

7. ASTM (2017). Standard Test Method for Determining the Initial Efficiency of Materials Used in Medical Face Masks to Penetration by Particulates Using Latex Spheres (ASTM International), Standard F2299/F2299M.

8. Rengasamy, S., Eimer, B., and Shaffer, R.E. (2010). Simple respiratory protection—evaluation of the filtration performance of cloth masks and common fabric materials against 20–1000 nm size particles. Ann. Occup. Hygene 54, 789–798.

9. Cooper, D.W., Hinds, W.C., and Price, J.M. (1983). Emergency respiratory protection with common materials. Am. Ind. Hyg. Assoc. J. 44, 1–6.

10. Konda, A., Prakash, A., Moss, G.A., Schmoldt, M., Grant, G.D., and Guha, S. (2020). Aerosol filtration efficiency of common fabrics used in respiratory cloth masks. ACS Nano 14, 6339–6347.

11. van der Sande, M., Teunis, P., and Sabel, R. (2008). Professional and home-made face masks reduce exposure to respiratory

infections among the general population. PLoS One 3, 1–6.

12. Cooper, D.W., Hinds, W.C., Price, J.M., Weker, R., and Yee, H.S. (1983). Expedient Methods of Respiratory Protection. II. Leakage Tests (Harvard School of Public Health), p. 47.

13. Brosseau, L.M., and Sietsema, M. (2020). Commentary: Masks-For-All for Covid-19 Not Based on Sound Data (University of Minnesota). https://www.cidrap.umn.edu/ news-perspective/2020/04/commentary-masks-all-covid-19-not-based-sound-data.

14. Tellier, R., Li, Y., Cowling, B., and Tang, J. (2019). Recognition of aerosol transmission of infectious agents: a commentary. BMC Infect. Dis. 19, 101.

15. OSHA (2004). Occupation Safety and Health Standards: Personal Protective Equipment (Occupational Safety and Health Administration), Rule number 1910.134.

16. TSI (2003). PortaCount Plus Model 8020: Operation and Service Manual (TSI Inc).

17. TSI (2002). Model 8026 Particle Generator: Operation and Service Manual (TSI Inc).

18. Farra, Y.M., Eden, M.J., Coleman, J.R., Kulkarni, P., Ferris, C.F., Oakes, J.M., and Bellini, C. (2020). Acute neuroradiological, behavioral, and physiological effects of nose-only exposure to vaporized cannabis in C57BL/6 mice. Inhalation Toxicol. https://doi.org/10.1080/08958378.08952020.01767237.

Supplemental Information

Quantitative Method for Comparative Assessment

of Particle Removal Efficiency of Fabric Masks

as Alternatives to Standard Surgical Masks for PPE

Amy V. Mueller, Matthew J. Eden, Jessica M. Oakes, Chiara Bellini, and Loretta A. Fernandez

SUPPLEMENTAL INFORMATION

Table SI1. Mask details, mean filtration efficiency ($\overline{x}$), standard deviation of mean filtration efficiency between replicates* (s_r), and standard deviation of filtration efficiency over one minute runs (s_t).

Sample	Description	worn as designed			worn with overlayer		
		$\overline{x}$	s_r	s_t	$\overline{x}$	s_r	s_t
N95-1		99.2%	0.4%	0.8%	-	-	-
N95-2	Makrite model 9500-N95	90.6%	5.9%	4.6%	95.2%	0.9%	4.7%
S-1	3M surgical mask model 1826	74.6%	4.1%	9.5%	90.3%	1.5%	3.9%
S-2	Keystone surgical mask model FM-EL-BLUE	59.3%	3.3%	13.0%	86.0%	3.2%	2.7%
S-3	Hong Da Wei Cai surgical mask labeled for medical use	53.4%	4.4%	12.6%	90.0%	6.0%	5.6%
O-1	surgical style 4 layer mask with black "charcoal" layer (no brand information available)	73.4%	4.1%	9.7%	86.8%	0.4%	5.2%
CS-1	cloth surgical-style mask with earloops and wired nose bridge, layers (3): two cotton quilting fabric and one Pellon interfacing fabric	58.6%	5.0%	11.6%	77.5%	6.2%	0.8%
CS-2	fabric surgical style mask with earloops, no wire at bridge of nose, layers: two cotton plain weave	28.2%	5.9%	24.3%	73.2%	1.4%	1.2%
CS-3	fabric surgical style mask with ties, wired nose bridge, layers (6): two Smartfab nonwoven fabric, two disposable baby wipe (dry), one massage table non-woven fabric cover, one meltblown filter (BFE85)	85.0%	1.3%	5.4%	81.3%	3.4%	7.9%
CS-4	fabric surgical style mask with ties, wired nose bridge, layers (2): two cotton duck	72.9%	8.8%	7.1%	78.5%	12.3%	6.7%
CS-5	fabric surgical style mask with ties, no wire at bridge of nose, layers (2): two layers of cotton twill (sold by Reformation clothing company at thereformation.com)	56.0%	3.9%	13.1%	66.9%	1.7%	10.2%

Table SI1 (cont.). Mask details, mean filtration efficiency ($\overline{x}$), standard deviation of mean filtration efficiency between replicates* (s_r), and standard deviation of filtration efficiency over one minute runs (s_t).

Sample	Description	worn as designed			worn with overlayer		
		$\overline{x}$	s_r	s_t	$\overline{x}$	s_r	s_t
CS-6	fabric surgical style mask with earloops, no wire at bridge of nose, layers (2): woven nylon	47.1%	2.3%	12.2%	56.8%	5.9%	8.7%
CC-1	commercially produced nuisance dust mask modified with cloth liner, layers (4): two Smartfab nonwoven fabric , one disposable baby wipe (dry), one meltblown filter (BFE84)	85.9%	6.3%	4.7%	89.3%	1.5%	3.8%
CC-2	commercially produced nuisance dust mask	60.3%	3.2%	10.4%	61.1%	2.8%	9.4%
CC-3	fabric cone-shaped mask with elastic head band and wired nose bridge, layers (6): two cotton muslin fabric, two disposable baby wipe (dry), one massage table cover non-woven fabric, one meltblown filter (BFE85)	86.2%	1.0%	5.5%	88.5%	0.9%	3.8%
CC-4	fabric cone-shaped mask with elastic head band, layers (6): two Smartfab nonwoven fabric, two disposable baby wipe (dry), one massage table non-woven fabric cover, one meltblown filter (BFE85)	89.1%	1.7%	3.4%	91.7%	2.8%	4.3%
CC-5	fabric cone-shaped mask with elastic head band, wired nose bridge, PM2.5 filter insert, layers (4, including pocket): three cotton muslin, one massage table non-woven fabric cover	80.2%	2.5%	7.1%	84.3%	2.5%	5.9%

Table SI1 (cont.). Mask details, mean filtration efficiency ($\overline{x}$), standard deviation of mean filtration efficiency between replicates* (s_r), and standard deviation of filtration efficiency over one minute runs (s_t).

Sample	Description	worn as designed			worn with overlayer		
		$\overline{x}$	s_r	s_t	$\overline{x}$	s_r	s_t
CC-6	fabric cone-shaped mask with elastic head band, layers (5): two Smartfab nonwoven fabric, one massage table non-woven fabric cover, two meltblown filter (BFE85)	90.7%	0.8%	3.1%	91.5%	1.1%	3.1%
CC-7	fabric cone-shaped mask with elastic head band, wired nose bridge, layers (4): two Smartfab nonwoven, one massage table non-woven fabric cover, two meltblown filter (BFE85)	85.3%	2.2%	4.6%	87.2%	0.9%	4.4%
CC-8	fabric cone-shaped mask with two sets of ties, wired nose bridge, layers (3): two cotton fabric, one non-woven polypropylene (recycled grocery bag)	82.6%	1.2%	5.7%	81.3%	2.4%	8.5%
CD-1	duck-bill shaped mask with elastic head band, wired nose bridge, layers (6): 4 cotton fabric, 2 Pellon interfacing	64.2%	11.0%	9.5%	80.2%	1.8%	6.3%
N only	woven nylon stocking	7.0%	2.5%	18.0%	-	-	-

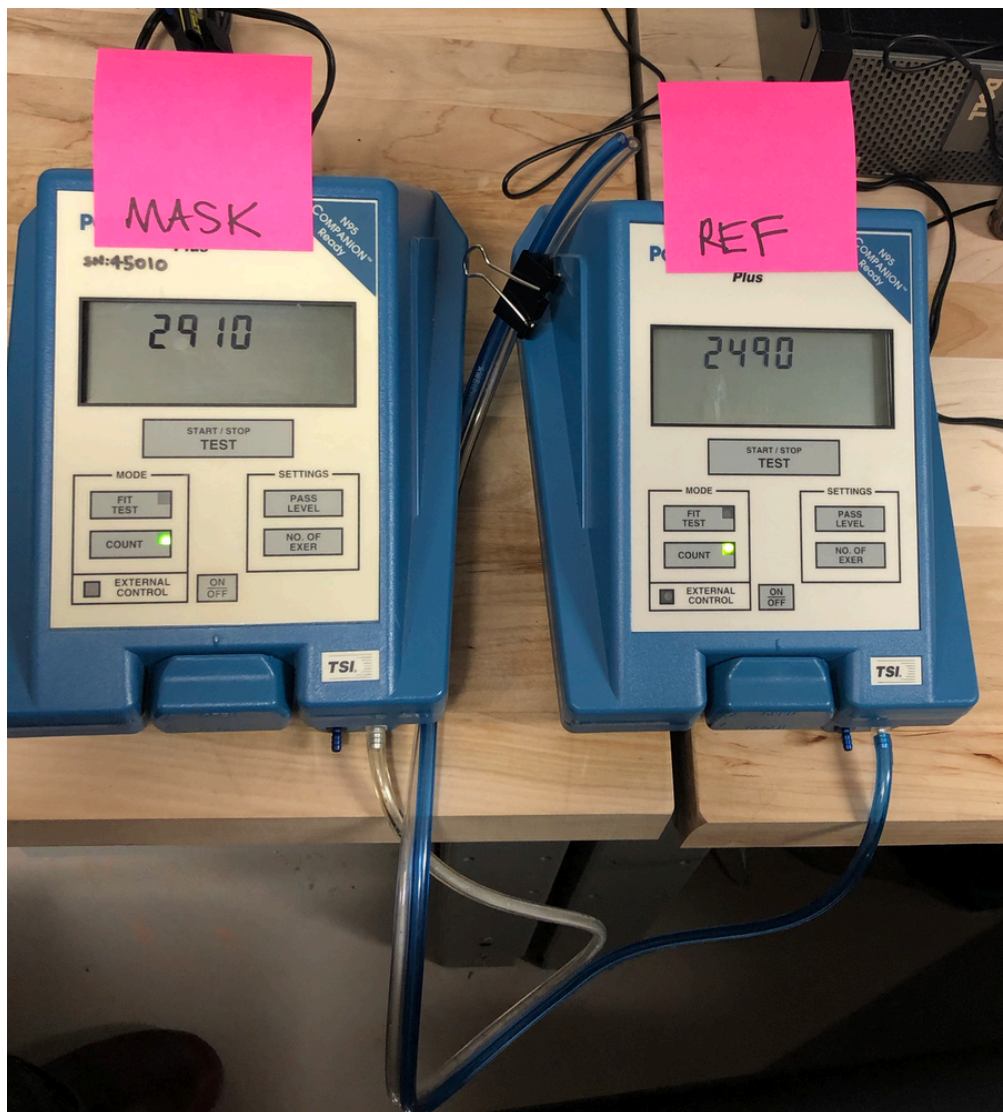* n=4 replicates for mask CS-1, all other masks n=3 replicates

Figure S1. Two TSI PortaCount model 8028 used in this work. Sample tubes are of equal length and are connected to right-hand ports labeled "sample". Instruments were operated in count mode with "Mask"-labeled instrument sampling air from inside the mask and "Ref"-labeled instrument sampling ambient air just outside of the mask.

N95-1 **N95-2** **S-1** **S-2**

O-1 **CS-1** **CS-2** **CS-3**

CS-4 **CS-5** **CS-6** **CC-1**

CC-2 **CC-3** **CC-4** **CC-5**

CC-6 **CC-7** **CC-8** **CD-1**

Figure S2. Gallery of mask images. Masks ordered by sample ID. Descriptions included in Table S1.

Additional and updated results are available through a web portal at masktestingatNU.com.